

2

AD-A210 500

SYNTHESIS AND PHYSICAL PROPERTIES OF  
POLY(PERFLUOROALKYLETHER)URETHANES

X-H. Yu<sup>\*</sup>, A.Z. Okkema<sup>1</sup>, and S.L. Cooper<sup>\*\*2</sup>

Material Science Program<sup>1</sup> and Department of Chemical Engineering<sup>2</sup>  
University of Wisconsin-Madison  
Madison, Wisconsin 53706

May 1989

\* Visiting Scholar from Nanjing University, People's Republic of China.

\*\* Author to whom correspondence should be addressed.

DTIC  
ELECTE  
JUL 25 1989  
S D D

DISTRIBUTION STATEMENT A  
Approved for public release;  
Distribution Unlimited

89 7 25 009

#### ABSTRACT

Polyurethane block copolymers were synthesized containing 33 and 50 wt% soft segment, and hard segments based on 4,4'-diphenylmethane diisocyanate (MDI) and either butanediol (BD) or N-methyldiethanolamine (MDEA) chain extender. The soft segments were mixtures of poly(tetramethylene oxide) (PTMO) and poly(perfluoroalkylether) (PFEG) glycols (Mn=1000 and 1900, respectively), ranging from 4 to 100 wt% PFEG. The PTMO polyol in one sample was substituted with a PTMO/ethylene oxide polyol (75:25 mole ratio) (Mn=1140). The MDEA-extended polymer was ionized using 1,3-propane sultone. The morphology, bulk, and surface properties of these polymers were evaluated by a variety of techniques. Differential scanning calorimetry and dynamic mechanical analysis showed that the incorporation of PFEG into the soft segment phase slightly enhanced the degree of phase separation. The ultimate tensile strength and elongation was reduced by the addition of PFEG. Chain extending with BD produced better phase separation and a higher tensile strength than the MDEA analog. In vacuum, surface enrichment of the low surface energy PFEG was observed for all the polymers, using electron spectroscopy for chemical analysis (ESCA). The dynamic contact angle results indicate that the polymer surfaces will rearrange in an aqueous environment to minimize their interfacial free energy.

## REPORT DOCUMENTATION PAGE

|  |       |   |  |  |   |                      |
|--|-------|---|--|--|---|----------------------|
| 1a. REPORT SECURITY CLASSIFICATION<br>None   |       |   | 1b. RESTRICTIVE MARKINGS<br>None   |  |   |                      |
| 2a. SECURITY CLASSIFICATION AUTHORITY<br>None  |       |   | 3. DISTRIBUTION / AVAILABILITY OF REPORT<br>Unlimited  |  |   |                      |
| 2b. DECLASSIFICATION / DOWNGRADING SCHEDULE<br>None  |       |   | 4. PERFORMING ORGANIZATION REPORT NUMBER(S)<br><br>Technical Report #21                      |  |   |                      |
| 6a. NAME OF PERFORMING ORGANIZATION<br>Dept. of Chemical Engineering<br>University of Wisconsin  |       |   | 6b. OFFICE SYMBOL<br>(if applicable)   |  | 7a. NAME OF MONITORING ORGANIZATION<br><br>Office of Naval Research |                      |
| 6c. ADDRESS (City, State, and ZIP Code)<br>1415 Johnson Drive<br>Madison, WI 53706   |       |   | 7b. ADDRESS (City, State, and ZIP Code)<br>800 N. Quincy St.<br>Arlington, VA 22217          |  |   |                      |
| 8a. NAME OF FUNDING / SPONSORING ORGANIZATION<br><br>ONR   |       | 8b. OFFICE SYMBOL<br>(if applicable)        |  | 9. PROCUREMENT INSTRUMENT IDENTIFICATION NUMBER<br><br>ONR N00014-83-K0423 |   |                      |
| 8c. ADDRESS (City, State, and ZIP Code)<br>800 N. Quincy St.<br>Arlington, VA 22217  |       |   | 10. SOURCE OF FUNDING NUMBERS  |  |   |                      |
|  |       | PROGRAM ELEMENT NO.                         | PROJECT NO.  | TASK NO.   | WORK UNIT ACCESSION NO.   |                      |
| 11. TITLE (Include Security Classification)<br><br>Synthesis and Physical Properties of Poly(perfluoroalkylether)urethanes   |       |   |  |  |   |                      |
| 12. PERSONAL AUTHOR(S)<br>Xue-Hai Yu, Ann Z. Okkema and Stuart L. Cooper   |       |   |  |  |   |                      |
| 13a. TYPE OF REPORT<br>Summary   |       | 13b. TIME COVERED<br>FROM 88/6/1 TO 89/5/31 |  | 14. DATE OF REPORT (Year, Month, Day)<br>89/5/30                           |   | 15. PAGE COUNT<br>41 |
| 16. SUPPLEMENTARY NOTATION<br>Submitted to   |       |   |  |  |   |                      |
| 17. COSATI CODES   |       |   | 18. SUBJECT TERMS (Continue on reverse if necessary and identify by block number)            |  |   |                      |
| FIELD  | GROUP | SUB-GROUP                                   | Polyurethanes, poly(perfluoroalkylether), mixed soft segment,<br>POLYMERS, ORGANIC CHEMISTRY |  |   |                      |
| 19. ABSTRACT (Continue on reverse if necessary and identify by block number)   |       |   |  |  |   |                      |
| <p>Polyurethane block copolymers were synthesized containing 33 and 50 wt% soft segment, and hard segments based on 4,4'-diphenylmethane diisocyanate (MDI) and either butanediol (BD) or N-methyldiethanolamine (MDEA) chain extender. The soft segments were mixtures of poly-(tetramethylene oxide) (PTMO) and poly(perfluoroalkylether) (PFEG) glycols (Mn=1000 and 1900, respectively), ranging from 4 to 100 wt% PFEG. The PTMO polyol in one sample was substituted with a PTMO/ethylene oxide polyol (75:25 mole ratio) (Mn=1140). The MDEA-extended polymer was ionized using 1,3-propane sultone. The morphology, bulk, and surface properties of these polymers were evaluated by a variety of techniques. Differential scanning calorimetry and dynamic mechanical analysis showed that the incorporation of PFEG into the soft segment phase slightly enhanced the degree of phase separation. The ultimate tensile strength and elongation was reduced by the addition of PFEG. Chain extending with BD produced better phase separation and a higher tensile strength than the MDEA analog. In vacuum, surface enrichment of the low surface energy PFEG was observed for all the polymers, using electron spectroscopy for chemical analysis (ESCA). The dynamic contact angle results indicate that the polymer surfaces will</p> |       |   |  |  |   |                      |
| 20. DISTRIBUTION / AVAILABILITY OF ABSTRACT<br><input checked="" type="checkbox"/> UNCLASSIFIED/UNLIMITED <input type="checkbox"/> SAME AS RPT <input type="checkbox"/> DTIC USERS   |       |   |  | 21. ABSTRACT SECURITY CLASSIFICATION<br>Unclassified                       |   |                      |
| 22a. NAME OF RESPONSIBLE INDIVIDUAL<br>Dr. Kenneth J. Wynne  |       |   |  | 22b. TELEPHONE (Include Area Code)   |   | 22c. OFFICE SYMBOL   |

19. rearrange in an aqueous environment to minimize their interfacial free energy.

## INTRODUCTION

Thermoplastic polyurethane elastomers are block copolymers consisting of alternating soft and hard segments. The soft segment is in a viscous or rubbery state, providing elastomeric character to the polymer. The hard segment is glassy or semicrystalline state and provides dimensional stability to the polymer by acting as a thermally reversible and multifunctional crosslink as well as a reinforcing filler. In the solid state the hard and soft segments of the copolymer aggregate into separate microdomains which results in an elevated rubbery plateau modulus and generally other enhanced physical properties.

In conventional segmented linear polyurethanes the soft segments are commonly low molecular weight (600-3000) polyether or polyester macroglycols. The hard segments generally consist of an aromatic diisocyanate which is chain extended with a low molecular weight diol to produce blocks with a distribution of molecular weights. The driving force for phase separation in these systems is the incompatibility of the soft and hard segments. The wide range of polymer morphologies and physical properties observed for polyurethane block copolymers, depends upon the composition and chemical structure of the hard and soft segments [1-3].

Polyurethane block copolymers based on polydimethylsiloxane (PDMS) soft segments are one example of well phase separated polyurethanes [4]. The polydimethylsiloxane segments are much more nonpolar than the hard segments, thus providing a strong driving force for phase separation [5]. Similarly, it is expected that the inclusion of a low molecular weight, nonpolar, polyperfluoroalkylether glycol into a

polyurethane should enhance the polymer's phase separation resulting in polyurethanes with interesting bulk and surface properties.

Fluorinated polymers are of interest due to their excellent thermal and oxidative stability [6], low surface tension, low friction [7,8], good chemical resistance [9], and their excellent oxygen permeability [10]. The ability of fluoropolymers to dissolve oxygen has led to their use in artificial blood applications [11]. The unique characteristics of fluorinated polymers are in part due to their low surface energy which results from the migration of the fluorine containing groups to the air-polymer interface providing a very hydrophobic surface.

Until recently, polyurethanes containing fluorinated alkylether soft segments have received little attention [8]. However, fluorinated polyurethanes prepared from conventional polyols but containing fluorinated diisocyanates and fluorinated short chain diols have been extensively studied [12-15]. Polyurethanes prepared from fluorinated diols generally lack the extensibility of their nonfluorinated analogs [12,13], while polyurethanes based on perfluoroalkyl diisocyanates are hydrolytically unstable [14]. Preliminary studies of polyurethanes containing fluorinated hydroxyl-terminated polyethers have shown that these polymers are both extensible and hydrolytically stable [14].

In this investigation, a series of eight polyetherurethane block copolymers containing 33 and 50 wt% soft segments and hard segments based on 4,4'-diphenylmethane diisocyanate (MDI), 1,4 butanediol (BD), or N-methyldiethanolamine (MDEA) were synthesized. Four of the polymers had soft segments composed of mixtures of polytetramethylene

oxide (PTMO) (MW=1000) and perfluoroalkyltetramethylene oxide glycol (PFEG) (MW=1900), ranging from 4 to 100 wt% PFEG. The PTMO macroglycol in one of the mixed soft segment polymers was replaced with a tetramethylene oxide/ethylene oxide polyol (75:25) (Mn=1140). The other four polymers contained pure PFEG soft segments with varying percentages of hard segment and type of chain extender. A zwitterionomer of the MDEA chain extended polymer was formed by the reaction of propane sultone with the tertiary nitrogen of MDEA.

The composition and sample designation for the polymers studied are described in Table I. An example of the sample designation for a mixed macroglycol polymer is ET-B33-F5. ET indicates the polymer is a polyetherurethane, B33 represents the 1,4 butanediol chain extender and the weight percentage of hard segment, while the F5 signifies that the soft segment contains 5 wt% PFEG with the remainder being PTMO (MW=1000). Similarly, M indicates the chain extender is MDEA and S8 indicates the weight percent of propane sultone substituted onto the tertiary nitrogen of the MDEA chain extender.

In this study, the microphase morphology, and physical properties of these polyurethanes were evaluated to determine what effect variations in the chain architecture such as the addition of PFEG into the PTMO soft segment, the percent hard segment, the type of chain extender, and the incorporation of ionic groups had on these properties.



|                      |                      |
|----------------------|----------------------|
| By _____             |                      |
| Distribution / _____ |                      |
| Availability Codes   |                      |
| Dist                 | Avail and/or Special |
| A-1                  |                      |

## EXPERIMENTAL METHODS

Synthesis

The fluorinated polyether glycol (PFEG) was kindly provided by Dr. E. Pechhold of E.I. du Pont de Nemours & Co. The macroglycol was purified prior to use by washing it 3 times with distilled water until pH 7 was attained, and then it was dried in a vacuum oven at 70°C for 24 hours. The MDI (Polysciences) was melted and pressure filtered at 60°C. Previous experiments in our laboratory have shown that pressure filtration and vacuum distillation are equivalent methods of purification for MDI. N,N-dimethylacetamide (DMAC) (Aldrich) was dehydrated over calcium hydride for two days and then vacuum distilled. Tetrahydrofuran (Aldrich) HPLC grade was kept over molecular sieves, while BD (Aldrich), stannous octoate catalyst (M&T chemicals), and 1,3 propane sultone (Aldrich) were used as received.

The segmented polyperfluoroalkyletherurethanes used in this study were synthesized by the two-step addition reaction. Solutions of PFEG and MDI were prepared in THF and N,N-dimethylacetamide (DMAC) respectively. The PFEG solution, containing 0.15 percent stannous octoate catalyst was slowly added to the stirred MDI solution at 60-70°C under dry argon. After an hour, the chain extender was added, and stirring was continued at 80-85°C. Chain extension with butanediol or MDEA required 6 hours. After a satisfactory molecular weight had been achieved, as determined by GPC analysis, the polymer was precipitated in hot distilled water, washed with ethyl alcohol, and then dried in a vacuum oven at 70-80°C for a minimum of two days. The polymer yield in all cases was greater than 90%. Polymers with mixed

soft segments (PFEG:PTMO) were synthesized by a similar procedure except that the PFEG solution was added first and allowed to react for one hour to avoid phase separation of the reactants. Then the PTMO in a DMAC solution was added and the reaction was continued for another hour.

Zwitterionization, as shown in Scheme I, was carried out on a portion of the MDEA-extended polymer by first dissolving it in DMAC. A stoichiometric amount of 1,3 propane sultone was added to the solution, and the reaction mixture was stirred at 40-50°C for 3 hours.

#### Sample Preparation

Films of the polyurethane block copolymers were spin cast from a 10% THF solution, dried in a vacuum oven at 65°C for two days, and then stored in a desiccator at room temperature. Film thickness ranged from 5  $\mu\text{m}$  to 200  $\mu\text{m}$  depending upon the requirements of a given experiment. The films were translucent to visible light.

Underwater contact angle evaluation was performed on samples prepared by coating the polymer onto the inner diameter of oxidized polyethylene (PE) tubing (Intramedic<sup>TM</sup>, Clay-Adams, 3.18 mm ID) following the protocol described by Lelah [16]. A 10 w/v% THF solution of each polymer was used for the coating procedure.

Films for electron spectroscopy for chemical analysis (ESCA) were cast from a 10 w/v% THF solution and then dried at 60°C in a vacuum oven for a minimum of 24 hours.

#### Bulk Characterization

An estimate of the molecular weight of the polymers was obtained

using a Waters Associates Model 501 high pressure gel permeation chromatograph using THF as the mobile phase. The average molecular weights were calculated on the basis of the molecular weight versus retention volume curve of monodisperse polystyrene standards.

Transmission infrared survey spectra were recorded with a Nicolet 7199 Fourier transform infrared spectrophotometer operated with a dry air purge. Two hundred scans at a resolution of  $2 \text{ cm}^{-1}$  were signal-averaged before Fourier transformation.

Thermal analysis was carried out on a Perkin-Elmer DSC-2 interfaced with a Perkin-Elmer Model 3600 Thermal Analysis Data Station (TADS) computer. The data processing unit allows subtraction of the background and normalization of the thermogram for sample weight. Temperature and enthalpy calibration were carried out using indium and mercury as standards. A heating rate of 20 K/min under a  $\text{N}_2$  purge was used.

Dynamic mechanical data were obtained using a microprocessor controlled Rheovibron DDV-II. All measurements were carried out under a  $\text{N}_2$  purge at a frequency of 110 Hz with a constant heating rate of  $3^\circ\text{C}/\text{min}$ .

Room temperature uniaxial stress-strain tests were performed using an Instron table model tensile testing device at a crosshead speed of 0.5 in/min. Dumbbell-shaped samples with a gauge length of 0.876 inches were stamped out using an ASTM D-1708 die.

#### Surface Characterization

ESCA spectra were obtained using a Physical Electronics PHI 5400 spectrometer with a 300 W, 15 kV magnesium anode. Widescan spectra

were obtained at a pass energy of 89.45 eV. High resolution spectra were recorded for all elements present, at a pass energy of 35.75 eV. The relative atomic percentage of each element at the surface was estimated from peak areas using atomic sensitivity factors specific for the PHI 5400. These factors account for the Scofield photoelectron cross sections [17], the kinetic energy dependence of the inelastic mean free path of emitted electrons, and the electron kinetic energy dependence of transmission function  $T(E_k)$  [18].

In order to analyze the chemical bonding of the carbon atoms, a higher resolution spectra of carbon was obtained at a pass energy of 17.90 eV. The high resolution  $C_{1s}$  spectrum for ET-B33-F67, is shown in Figure 1, and is representative of the other polymer spectra. The  $C_{1s}$  high resolution spectrum was smoothed, and then using a van Cittert routine [19] available in the PHI 5400 computer software, the spectrum was deconvoluted to account for the instrument loss function. The resulting spectrum consists of five peaks which were curve fit using a combination of Gaussian and Lorentzian peak shapes. The five peaks correspond to aliphatic and aromatic carbon (C-C, C-H) referenced at 285 eV [20,21], carbon singly bonded to oxygen at approximately 286.5 eV, and carbon doubly bonded to oxygen (C=O) at approximately 290 eV. The high electronegativity of the fluorine atom results in the higher binding energies of the fluorine substituted carbons, with the photoemission peak at 292.0 eV due to carbon bonded to two fluorine atoms ( $CF_2$ ) and the highest binding energy peak at 294.5 eV attributed to carbon bonded to three fluorine atoms ( $CF_3$ ) [21,22].

Underwater contact angle measurements were made using the technique of Hamilton [23], modified for use on curved surfaces [16].

The surfaces were equilibrated with double-distilled, deionized water for 24 hours prior to the collection of data. A minimum of ten measurements were used to calculate the average surface-water-air and surface-water-octane contact angles.

Dynamic contact angle measurements were obtained using a Cahn Surface Analyzer. Polymer coated coverslips were immersed and subsequently drawn out of high purity water at the speed of  $21 \text{ mm}^{-1}$ . The interfacial tension versus immersion depth curve was obtained and the advancing and receding angles were calculated from the curves [Andrade].

## RESULTS AND DISCUSSION

### Synthesis

According to the data generously provided by Dr. Pechhold, PFEG has a molecular weight,  $M_n=1900$ , and a fluorine content of 48.3 wt%. As shown in Scheme 2, the macroglycol is composed of a polyether backbone with a short pendant perfluoroalkyl side group.

A mixture of solvents, THF and DMAc, was used in the synthesis procedure to avoid macrophase separation of the reactants due to their different solubilities. These reactants were miscible throughout the synthesis as indicated by the clarity of the solution. The fluorine-containing polyurethanes were soluble in THF and DMAc.

The GPC analysis of these polymers was performed to verify that a reasonable molecular weights were obtained. The number average molecular weights are shown in Table I.

### Infrared Spectroscopy

The transmission infrared spectra for ET-B33-F0, ET-B33-F14 and ET-B33-F67 are shown in Figure 2 and are representative of the other samples. The incorporation of PFEG into the polymer backbone was verified by the two C-F absorbance bands at  $1152\text{ cm}^{-1}$  and  $1208\text{ cm}^{-1}$  [24] shown in Figure 2. As expected the intensity of the C-F absorbance peaks increased with the wt% PFEG in the polymer backbone. The other absorbance peaks in the IR spectra are representative of a typical polyetherurethane block copolymer.

In polyetherurethanes hydrogen bonding can occur between the urethane N-H groups and the hard segment carbonyl oxygen and alkoxy oxygen along with the soft segment ether oxygen [Knutson, K. (24) and West (25)]. The absence of an absorbance peak at  $3450\text{ cm}^{-1}$  indicates that nearly all the N-H groups are hydrogen bonded.

The ratio of the hydrogen bonded urethane carbonyl absorbance at  $1700\text{ cm}^{-1}$  to the free carbonyl absorbance at  $1732\text{ cm}^{-1}$  provide a qualitative estimation of the degree of phase separation in polyurethanes [Knutson (24)]. An increase in the bonded to free carbonyl ratio indicates an increase in the phase separation of the polymer. A decrease in the carbonyl ratio, however, may result from the urethane N-H hydrogen bonding with either the polyether oxygen or the urethane alkoxy oxygen.

As shown in Table X the incorporation of PFEG at all levels in the polymers containing 33 wt% hard segment lowered the ratio of bonded to free carbonyls relative to the ET-B33-F0. The decrease in bonded to free carbonyl ratio is not correlated with the PFEG wt% in

the polymer. ET-B33-F9 and ET-B33-F9-EO8 have lower ratios than ET-B33-F14 and ET-B33-F67. The reduction in the number of bonded carbonyls may be hypothesized to result from enhanced phase mixing of the PTMO macroglycol and hard segment induced by the nonpolar nature of the fluorocarbon. It seems unlikely that PFEG macroglycol and hard segment phase would be miscible. Alternatively, the PFEG may be promoting the hydrogen bonding of the N-H groups to the hard segment alkoxy oxygens rather than the urethane carbonyl.

For the PFEG soft segment polymers ET-B50-F50 has a higher bonded to free carbonyl ratio than ET-B33-F67 due to the greater number of carbonyls.

#### Thermal Analysis

Representative DSC curves for the first heating of the PTMO-based, PFEG-based, and the mixed polyol soft segment polymers, ET-B33-F0, ET-B33-F14, and ET-B33-F67 respectively are shown in Figure 3. The thermal transition results are summarized in Table II. All the polymers have a glass transition temperature ( $T_g$ ) and two endotherms attributed to the disruption of short and long range order of the hard segment domains.

The glass transition temperatures for the soft segment constituents, as pure homopolymers, are  $-85^\circ\text{C}$  for PTMO [25], approximately  $-46^\circ\text{C}$  for PEO [26] and  $-59^\circ\text{C}$  for PFEG, as determined using DSC. The thermal transitions of block copolymers are altered from the homopolymer transition temperatures due to mobility restrictions resulting from covalent bonding of hard and soft segments [27].

The addition of higher Tg PFEG segments should increase the glass transition of the polymer relative to ET-B33-Fo. Tg's for the theoretically mixed miscible soft segment components, as calculated using the Fox equation [z], should increase by 2.6 to 7.1° with increasing PFEG content. Mixing of the hard segment phase with the mixed macroglycol soft segments would further increase the Tg. Since the Tg's measured using DSC do not significantly change relative to the PTMO analog, ET-B33-F0, there must be an increase in phase separation compensating for the increase in soft segment Tg.

Further evidence of this improved phase separation is the slight increase in the long-range order hard segment domain disordering temperatures as shown in Table II. The short-range order endotherms are dependent on the polymer's thermal history and not on soft segment-hard segment interactions. The incorporation of 9wt% PFEG appears to reduce the long-range order of the hard segments as indicated by the smaller magnitude of the high temperature endotherm and the broader short range order endotherm. However, the higher dissociation temperature of the long-range packing endotherm suggest that the packing of some of the hard segments are approaching a microcrystalline state. The addition of ethylene oxide in the soft segment, ET-B33-F9-E08, further enhanced the packing of these hard segments as indicated by the much higher disordering temperature.

As shown in Table II, the relatively high Tg for ET-B33-F67 compared with the Tg of the PFEG polyol indicates there is some hard segment dispersed in the soft segment phase. From a surface free energy perspective, the relatively polar polyether backbone of the PFEG polyol should be compatible with the hard segment phase. The

nonpolar fluorine-containing pendant group would be expected to orient away from the hard segment. The higher  $T_g$  of ET-B50-F50 compared with ET-B33-F67 indicated that it has a more phase mixed morphology. The increase in phase mixing with hard segment content is attributed to the greater number of single MDI unit hard segments which are soluble in the soft segment phase [27]. The higher  $T_g$  and absence of high temperature endotherm for the MDEA chain extended polymer, ET-M34-F66, indicated it was more phase mixed than its BD-extended analog. The methyl pendant group of the MDEA disrupts the hard segment packing, thereby enhancing phase mixing [28,29]. Ionization of the MDEA chain extender polymer, promotes phase separation as indicated by the dramatic decrease in the soft segment phase  $T_g$  and the appearance of a short range order endotherm at  $117^\circ$ . The propyl sulfonate groups increase the polarity difference between the segments thereby enhancing phase separation. These results are in agreement with previous studies investigating MDEA chain extended ionomers [Miller, J. Macromol. Sci. phys. B22(2) 321-341(1983)].

#### Dynamic Mechanical Analysis

The dynamic mechanical analysis (DMA) results for the polymers are presented in Figures 4 and 5 and the transition data are summarized in Table II. The low temperature transition ( $\gamma$  peak) and the glass transition temperature of the soft segment ( $\alpha$  peak), are determined from the peak positions in the loss modulus ( $E''$ ) curve. In general the transition temperatures determined by DMA are higher than the values determined by DSC, due to the difference in the time scale of the experiments [3,32,33]. The results for all the materials are in

accord with and support the conclusions drawn from the DSC data discussed in the previous section.

The low temperature transition ( $\gamma$  peak) is attributed to the local mode motion of primarily PTMO in the mixed soft segment polymers and the butanediol segments for the 100% PFEG soft segment polymers. In agreement with the DSC results, the  $T_g$ s for the mixed soft segment polyurethanes are either the same or slightly lower than the PTMO-based polymer ET-B33-F0. These results indicate the addition of PFEG enhanced the degree of phase separation in the polymers. The DMA curves for ET-B33-F0 and ET-B33-F14 shown in Figure 5 are similar to the curves for ET-B33-F5 and ET-B33-F9 (not shown). The rubbery plateau modulus was slightly reduced with increasing incorporation of PFEG.

For the 100% PFEG polymers, ET-B50-F50 appears more phase mixed than ET-B3-F67 as observed in the DSC data. In addition, as shown in Figure 4, there is an enhancement in the rubbery modulus and a broadening of the  $\alpha$  peak for ET-B50-F50 compared with ET-B33-F67, due to an increase in the size and interconnectivity of the hard segment domains. The higher  $T_g$  for the MDEA-extended polymer indicates it was more phase mixed than its BD-extended analog. Ionization of the MDEA chain extended polymer improves domain cohesion and phase separation resulting in an enhanced plateau modulus as well as extending it to higher temperatures.

The thermal analysis results suggest that the decrease in bonded carbonyl to free carbonyl is due to the hydrogen bonding of the alkoxy groups in the hard segment since there is an increase in phase separation.

### Tensile Properties

The stress-strain curves for the mixed soft segment polyurethanes and the pure PFEG soft segment polyurethanes are shown in Figures 6 and 7 respectively. The strength and elastic properties of the polyurethanes are listed in Table III.

For the mixed soft segment polyurethanes, as the PFEG content increases the mechanical properties decrease, as shown in Figure 6. The stress-strain behavior of ET-B33-F14 (not shown) is similar to ET-B33-F9. The decrease in mechanical strength, modulus, and elongation is attributed to the bulky perfluorinated side group of PFEG, which prevents crystallization of the soft segment upon extension and increases interchain separation. The decrease in Young's modulus and 100% tensile modulus with PFEG content is in agreement with the DMA plateau modulus discussed in the previous section. It has been shown that polyurethanes containing highly incompatible soft segments generally possess inferior tensile properties [35]. It is not clear whether this is due to the reduction of strain induced crystallization or the presence of very sharp phase boundaries in these systems. The incorporation of PEO into the soft segment of ET-B33-F9-E08 dramatically decreases the ultimate strength and elongation of the polymer while increasing the Young's modulus.

As expected for the pure PFEG soft segment polymers, the ultimate strength and Young's modulus are highest for the polymer containing the highest concentration of hard segment, ET-B50-F50, which exhibits the stress-strain behavior of a tough plastic. The increase in tensile strength is attributed to an increase in the hard segment block length

and content, along with the more interconnected hard segment domain morphology [27,34]. For the MDEA-extended polymers, the decrease in the stress to failure and the tensile modulus is due to the inability of the MDEA based hard segments to crystallize. Upon ionization the enhancement of the polarity difference between the segments and the formation of ionic aggregates enhance phase separation thereby increasing the strength and modulus of the polymer. These results indicate that hard-domain cohesiveness is a major factor determining the tensile properties of these 100% PFEG soft segment polyurethanes.

#### Surface Analysis

Electron spectroscopy for chemical analysis (ESCA) was used to investigate the composition and chemistry of the air-cast surfaces of each polymer. The element atomic percentages in Table IV were calculated from the bulk polymer stoichiometries and determined from the ESCA analysis performed at a take off angle of 45°.

The fluorine and the fluorocarbon,  $CF_2$  and  $CF_3$ , photoemission peaks are representative of the soft segment phase while the nitrogen and carbonyl peaks are representative of the hard segment phase. The trends in the atomic percentages of these peaks, therefore, are related to the morphology of the polymer surface. Fluorine has a high photoemission cross section and high electronegativity which enhances its detectability. The intensity of the  $N_{1s}$  signal is weak thus caution must be used when interpreting these results.

Fluorine-containing molecules generally have very low surface energies, thus it is expected that the PFEG segment of the polyurethane will orient at the air interface to minimize the

interfacial energy. As indicated in Table IV, the fluorine concentration for all of the mixed polyol polyurethanes is much greater than the bulk concentration indicating that the PFEG soft segment is enriched at the surface. A measure of the level of surface enhancement of the PFEG macroglycol is given by the difference between the experimental and bulk fluorine concentrations. This quantity is referred to as  $\Delta F$ . The surface enrichment of PFEG increases with increasing PFEG content for the mixed soft segment polymers. The addition of ethylene oxide into the tetramethylene oxide macroglycol increase the polyols polarity. The increased polarity of this macroglycol promotes the enrichment or segregation of PFEG to the surface as indicated by the higher  $\Delta F$  value for ET-B33-F9-EO8 relative to ET-B33-F9.

The nitrogen concentrations for the mixed polyol polymers are significantly lower than the bulk values. The higher percentage of nitrogen and carbonyl at the ET-B33-F9 surface compared with ET-B33-F5 and -14 is somewhat puzzling. These results indicate there is more hard segment present at these surfaces, however the soft segment concentration does not correspondingly decrease. The incorporation of EO into the soft segment greatly enhances the amount of hard segment, does both N and C=O increase at both surfaces relative to ET-B33-F9.

For all the 100% PFEG soft segment polymers the fluorine content at the surfaces is significantly higher than the bulk concentration. At the surface ET-B50-F50 has a lower fluorine and fluorocarbon concentration than ET-B33-F67, which correlates with their bulk fluorine concentrations. The fluorine and fluorocarbon concentrations are approximately equal at both surfaces for the relatively phase

mixed MDEA chain extended polymer, ET-M34-F66. Propyl sulfonate incorporation slightly decreases the surface fluorine content relative to ET-M34-F66, probably due to the polarity of the sulfonic acid groups. In addition 0.2 atomic% sulfur was detected on the surface of the sulfonated polymer.

Silicon contamination probably in the form of siloxane, is present in all the polyurethanes studied.

#### Contact Angle

Underwater contact angle results, using air and octane as probe fluids, describe the surface morphology of the polymers in an aqueous environment. The average surface-water-air and surface-water-octane contact angles are listed in Table V.

As expected the incorporation of PFEG into the PTMO based polyurethanes increases the hydrophobicity of the polymer surface. As indicated by the contact angles for ET-B33-F9 and ET-B33-F14, the hydrophobic character of the surface appears to level out at about 9 wt% incorporation. Similar results have been observed by Ito and coworkers [36] for polyurethanes containing greater than 7 wt% fluorinated diol chain extender and a fluorinated polyether.

As illustrated by the decrease in the surface-water-air and surface-water-octane contact angles of ET-B33-F9-EO8, the incorporation of the hydrophilic PEO macroglycol into the soft segment increases the hydrophilicity of the polymer surface compared with ET-B33-F9.

The air and octane contact angles for ET-B33-F67 and ET-B50-F50 are approximately equal. This result is somewhat surprising since

ET-B50-F50 contains 17 wt% more polar hard segment than ET-B33-F67. The air contact angles for the 100% PFEG soft segment BD-chain extended polymers are similar to the air contact angles of the mixed soft segment polymers PEU-33-F-8 and -14 even though these polymers contain significantly less fluorocarbon. These results suggest that the effect of PFEG on the polarity of the polymer surface may be complicated by the complex structure of the PFEG macroglycol. In addition, the surface morphology of these polymers is also affected by the change in bulk morphology which changes roughly from a soft segment matrix with hard segment inclusions for ET-B33-F67, to co-continuous morphology or a hard segment matrix with soft segment inclusions for ET-B50-F50.

The MDEA chain extended polymer PEU-MDEA-33 is significantly more hydrophilic than the BD chain extended analog probably due to the phase mixed morphology of the polymer. As expected, the incorporation of sulfonic acid groups significantly enhances the hydrophilicity of the polymer.

#### Dynamic Contact Angle

The polarity of the casting environment does not significantly affect the fluorine concentrations of the polymers which have only PFEG as the soft segment. The hard segment surface concentration however, is somewhat influenced by the casting environment. As indicated by the nitrogen and carbonyl concentrations the hard segment surface content follows the same trend as the fluorine and fluorocarbon concentrations indicating the surfaces may be phase mixed. From a surface energetics perspective, the more polar hard

segment would be expected to segregate to the water surface.

#### CONCLUSIONS

A novel series of poly(perfluoroalkylether)urethanes, which possess interesting bulk and surface properties, have been synthesized. The incorporation of the perfluoroalkyl macroglycol into the polyurethane structure was verified by the presence of two C-F absorbance peaks observed in the polymer's IR spectra. As indicated by GPC analysis these perfluorinated polyurethanes have a satisfactory molecular weight of approximately 40,000.

The bulk property results indicate that the morphology and mechanical properties of the polymers containing 100% PFEG soft segment are strongly dependent on the percentage of hard segment and the type of chain extender used. The incorporation of PFEG enhanced the phase separation and hard segment crystallinity. The MDEA chain extended polymer is more phase mixed than a BD-extended analog. Substitution of propyl sulfonate groups onto the MDEA chain extended polymer enhanced phase separation. The highest hard segment containing polymer, ET-B50-F50, exhibited the stress-strain behavior of a tough plastic, while the other polymers show typical elastomeric behavior. The tensile properties are lower for the more phase mixed MDEA chain extended polymer.

The surface of the polymers containing 100% PFEG soft segment is also enhanced in the PFEG soft segment. The polarity of the polymer surface appears to be controlled by several factors; the bulk

morphology of the polymer, the polarity of the casting and testing environment and the complex amphipathic structure of PFEG.

The tensile properties of the mixed macroglycol polyurethanes were slightly reduced by increasing PFEG content (5 to 14 wt%), while the elongation remained unaffected. As indicated by thermal and dynamic mechanical analysis these polymers are relatively well phase separated. The incorporation of PFEG increases the hard segment crystallinity of all the polymers.

The incorporation of PFEG, even as low as 5 wt%, resulted in a dramatic increase in the concentration of fluorine at the polymer surface as determined using ESCA. The atomic percentage of fluorine is greatest for ET-B33-F14. The polarity of the casting environment appears to have the greatest affect on the polymer blocks that have similar polarities and provide the driving force for the reorientation of the polymer surface. The hydrophobicity of the polymer surface plateaus at a PFEG content of 9 wt% and greater as indicated by the static contact angle results.

The incorporation of PEO into the soft segment decreased the tensile properties and increased the hydrophilicity of the polymer surface.

Polyurethanes based on perfluoroalkyl glycol soft segments can be readily synthesized and possess surface and bulk properties which make them interesting as elastomers, coatings, biomaterials, and other polymer applications.

#### ACKNOWLEDGEMENTS

The authors acknowledge Robert Schumacher for his assistance in

obtaining the bulk property data. The work was supported by ONR  
Contract N00014-83-K0423.

## REFERENCES

1. G.M. Estes, S.L. Cooper, and A.V. Tobolsky, J. Macromol. Sci. Rev. Macromol. Chem., 4, 313 (1970).
2. A. Noshay and J.E. McGrath, Block Copolymers: Overview and Critical Survey, Academic, New York, 1977.
3. P.E. Gibson, M.A. Vallance, and S.L. Cooper, in Developments in Block Copolymers, I, Goodman, Ed., Appl. Sci. Ser., Elsevier, London, 1982.
4. Yu Xue-Hai, M.R. Nagarajan, T.G. Grasel, P.E. Gibson, and S.L. Cooper, J. of Polymer Science: Polymer Physics Edition, 23, 2319 (1985).
5. R. Ramharach, and T.H. Nguyen, J. Polym. Sci. Polym. Let., 25, 93 (1987).
6. F. Gosnell, and J. Hollander, J. Macromol. Sci.-Phys., B1(4), 831 (1967).
7. E.G. Shafrin and W.A. Zisman, J. Phys. Chem., 64, 519 (1960).
8. J.R. Griffith and J.D. Bultman, Ind. Eng. Chem. Prod. Res. Dev., 17, 8 (1978).
9. E.P. Wesseler, R. Iltis, and L.C. Clark, Jr., J. Fluorine Chem., 9, 137 (1977).
10. D.L. Hunston, J.R. Griffith, and R.C. Bowers, Ind. Eng. Chem. Prod. Res. Dev., 17, 8 (1978).
11. J.G. Reiss, and M. Le Blanc, Angew. Chem. Int. Ed. Engl., 17, 621 (1978).
12. J. Hollander, F.D. Trischler, and E.S. Harrison, Polym. Prepr. Am. Chem. Soc. Div. Polym. Chem., 8, 1149 (1967).
13. T.M. Keller, J. Polym. Sci: Polym. Chem. Ed., 23, 2557 (1985).
14. J. Hollander, F.D. Trischler, and R.B. Gosnell, J. Polym. Sci: Part A-1, 5, 2757 (1967).
15. S.C. Yoon and B.D. Ratner, Macromolecules, 19, 1068 (1986).
16. M.D. Lelah, T.G. Grasel, J.A. Pierce, and S.L. Cooper, J. Biomed. Mater. Res., 19, 1011 (1985).
17. J.H. Scofield, J. Electron. Spectrosc. Relat. Phenom., 8, 129 (1976).

18. A. Proctor and D.M. Hercules, Appl. Spectrosc., 38(4), 505 (1984).
19. P.A. Jansson, Deconvolution with Applications in Spectroscopy, Academic Press, Orlando, Florida, 1984.
20. H.R. Thomas and J.J. O'Malley, Macromolecules, 12, 323 (1979).
21. D.T. Clark, W.J. Feast, D. Kilcast, and W.K.R. Musgrave, J. Polym. Sci: Polym. Chem. Ed., 11, 389 (1973).
22. A. Takahara, N. Higashi, T. Kunitake, and T. Kajiyama, Macromolecules, 21, 2443 (1988).
23. W.C. Hamilton, J. Colloid Interface Sci., 40, 219 (1972).
24. J. Brandrup and E.H. Immergut, Eds., Polymer Handbook, Wiley, New York, 1975.
25. J.A. Fraucher, and J.V. Koleske, Polymer, 9, 44 (1968).
26. K.K.S. Hwang, S.B. Lin, S.T. Tsay and S.L. Cooper, Polymer, 25, 947 (1984).
27. J.A. Miller, S.B. Lin, K.K.S. Hwang, K.S. Wu, P.E. Gibson, and S.L. Cooper, Macromolecules, 18, 32 (1985).
28. T.A. Speckhard, K.K.S. Hwang, C.Z. Yang, W.R. Laupan, and S.L. Cooper, Macromolecules, B23(2), 175 (1984).
29. K.K.S. Hwang, C.Z. Yang and S.L. Cooper, Polym. Eng. and Sci., 21, 1027 (1981).
30. O. Olabisi, L.M. Robeson and M.T. Shaw, Polymer-Polymer Miscibility, Academic Press, New York, 282 (1979).
31. R.W. Seymour and S.L. Cooper, Macromolecules, 6, 48 (1973).
32. J.D. Ferry, Viscoelastic Properties of Polymers, John Wiley & Sons, New York, 280 (1980).
33. J.J. Alkonis and W.J. MacKnight, Introduction to Polymer Viscoelasticity, John Wiley & Sons, New York, 57 (1983).
34. C. Hepburn, Polyurethane Elastomers, Applied Science, London, (1982).
35. T.A. Speckhard and S.L. Cooper, Rubber Chem. and Tech., 59, 405 (1985).
36. Y. Ito, T. Kashiwagi, S.Q. Liu, L.S. Liu, Y. Kawamura, Y. Iguchi, Y. Imanishi, in Proceedings of the 2nd International Symposium on Artificial Heart and Assist Device, Tokyo, Japan, Aug. 1987, Springer-Verlag, Tokyo.

## FIGURE CAPTIONS

Figure 1. High resolution Cls spectra of ET-B33-F67.

Figure 2. Transmission IR spectra for ET-B33-F67, ET-B33-F14, and ET-B33-F0.

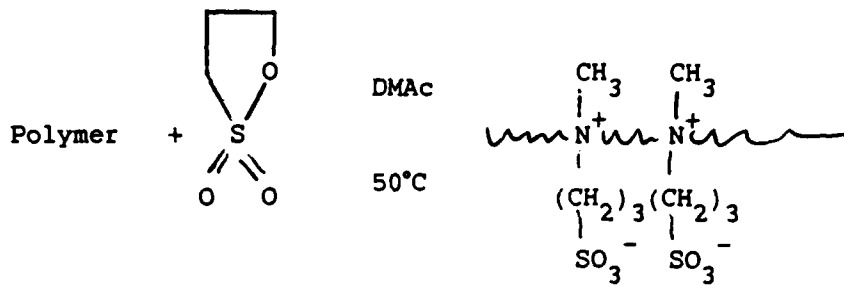
Figure 3. DSC curves for ET-B33-F0, ET-B33-F14, ET-B33-F67.

Figure 4. Dynamic mechanical curves of the 100% PFEG soft segment polymers.

Figure 5. Dynamic mechanical curves of the mixed soft segment polymers.

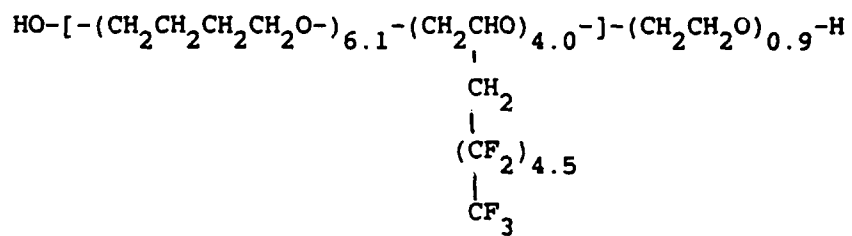
Figure 6. Stress strain curves for the 100% PFEG soft segment polymers.

Figure 7. Stress strain curves for the mixed macroglycol soft segment polymers.



Scheme 1: Synthetic scheme for zwitterionization of the MDI/MDEA/PFEG

polymer.



Scheme 2: Structure of perfluoroalkylether polyol.

TABLE I  
MATERIAL CHARACTERIZATION

| Sample Code   | Composition  | Molecular<br>Weight |
|---------------|--|---------------------|
| ET-B33-F0     | 33 wt% MDI/BD,<br>67 wt% PTMO (1000 MW),   | 41,000              |
| ET-B33-F5     | 33 wt% MDI/BD,<br>62 wt% PTMO (1000 MW),<br>4.8 wt% FPEG (1899 MW)   | 40,000              |
| ET-B33-F9     | 33 wt% MDI/BD,<br>58 wt% PTMO (1000 MW),<br>9.4 wt% FPEG (1899 MW)   | 35,000              |
| ET-B33-F14    | 33 wt% MDI/BD,<br>53 wt% PTMO (1000 MW),<br>13.8 wt% FPEG (1899 MW)  | 42,000              |
| ET-B33-F9-E08 | 33 wt% MDI/BD,<br>58 wt% PTMO/EO polyol<br>consisting of 75:25 mole ratio<br>(8 wt% EO) (1140 MW),<br>9.4 wt% FPEG (1899 MW) | 32,000              |
| ET-B50-F50    | 50 wt% MDI/BD,<br>50 wt% FPEG (1899)   | 40,000              |
| ET-B33-F67    | 33 wt% MDI/BD,<br>67 wt% FPEG (1899)   | 38,000              |
| ET-M34-F66    | 34 wt% MDI/MDEA,<br>66 wt% FPEG (1899)   | 35,000              |
| ET-M34-F66-S8 | PEU-MDEA-34 reacted with<br>8 wt% propane sultone  | -                   |

\* GPC peak value

TABLE II  
TRANSITION DATA

DIFFERENTIAL SCANNING CALORIMETRY

| Sample         | T <sub>g</sub><br>Midpoint<br>(°C) | Glass<br>Transition<br>Range (°C) | High Temperature<br>Endotherm<br>(°C) |
|----------------|------------------------------------|-----------------------------------|---------------------------------------|
| ET-B33-F0      | -49                                | 47                                | 162                                   |
| ET-B33-F5      | -48                                | 51                                | 162                                   |
| ET-B33-F9      | -48                                | 40                                | 170                                   |
| ET-B33-F14     | -50                                | 27                                | 164                                   |
| ET-B33-F9-EO8  | -48                                |                                   | 179                                   |
| ET-B50-F50     | -10                                | 13                                | 142                                   |
| ET-B33-F67     | -17                                | 38                                | 160                                   |
| ET-M34-F66     | -12                                | 25                                | 166                                   |
| ET-M34-F66-S8  | -22                                | 46                                | -                                     |
| FPEG (1899 MW) | -59                                | 11                                |                                       |

DYNAMIC MECHANICAL PROPERTIES

| $\gamma$ Peak<br>(°C) | T <sub>g</sub><br>(°C) |
|-----------------------|------------------------|
| -131                  | -32                    |
| -128                  | -35                    |
| -128                  | -31                    |
| -128                  | -32                    |
| -128                  | -30                    |
| -133                  | 10                     |
| -130                  | -14                    |
| -130                  | -2                     |
| -132                  | -8                     |

TABLE III  
MECHANICAL PROPERTIES

| Sample        | Young's<br>Modulus<br>(MPa) | 100%<br>Secant<br>Modulus<br>(MPa) | Ultimate<br>Stress<br>(MPa) | Percent<br>Elongation<br>at Break |
|---------------|-----------------------------|------------------------------------|-----------------------------|-----------------------------------|
| ET-B33-F0     | 37.1                        | 7.5                                | 31.6                        | 560                               |
| ET-B33-F5     | 30.3                        | 6.8                                | 13.8                        | 450                               |
| ET-B33-F9     | 30.0                        | 6.3                                | 12.9                        | 440                               |
| ET-B33-F14    | 25.5                        | 4.9                                | 12.5                        | 430                               |
| ET-B33-F9-EO8 | 40.6                        | -                                  | 5.4                         | 80                                |
| ET-B50-F50    | 184.7                       | -                                  | 21.6                        | 60                                |
| ET-B33-F67    | 28.9                        | -                                  | 6.6                         | 40                                |
| ET-M34-F66    | 9.1                         | 2.0                                | 3.1                         | 130                               |
| ET-M34-F66-S8 | 26.1                        | 10.2                               | 11.3                        | 110                               |

TABLE IV

ESCA ANALYSIS  
(Atomic Percent)

| MATERIAL      | F    |     | CF <sub>2</sub> |     | CF <sub>3</sub> |     |
|---------------|------|-----|-----------------|-----|-----------------|-----|
|               | Bulk | Exp | Bulk            | Exp | Bulk            | Exp |
| ET-B33-F0     | -    | -   | -               | -   | -               | -   |
| ET-B33-F5     | 2    | 26  | 0.6             | 5.9 | 0.1             | 1.7 |
| ET-B33-F9     | 3    | 30  | 1.3             | 9.0 | 0.3             | 1.8 |
| ET-B33-F14    | 5    | 35  | 1.9             | 8.0 | 0.4             | 2.1 |
| ET-B33-F9-E08 | 3    | 33  | 1.2             | 7.4 | 0.3             | 2.0 |
| ET-B50-F50    | 18   | 34  | 7.0             | 9.7 | 1.5             | 4.6 |
| ET-B33-F67    | 25   | 36  | 9.5             | 9.7 | 2.1             | 2.3 |
| ET-M34-F66    | 25   | 34  | 9.4             | 9.1 | 2.1             | 2.1 |
| ET-M34-F66-S8 | 23   | 29  | 8.7             | 8.2 | 1.9             | 2.1 |

| N    |     | C=O  |     | Si  | S    |     |
|------|-----|------|-----|-----|------|-----|
| Bulk | Exp | Bulk | Exp | Exp | Bulk | Exp |
| 4.4  | 3.2 | 4.4  | 3.8 | 1.5 | -    | -   |
| 4.4  | 2.6 | 4.4  | 1.9 | 0.0 | -    | -   |
| 4.3  | 1.6 | 4.3  | 1.0 | 0.0 | -    | -   |
| 4.2  | 1.9 | 4.2  | 1.2 | 0.1 | -    | -   |
| 4.0  | 2.2 | 4.0  | 2.4 | 0.0 | -    | -   |
| 4.6  | 3.0 | 4.7  | 3.2 | 0.1 | -    | -   |
| 3.2  | 2.4 | 3.2  | 2.2 | 0.1 | -    | -   |
| 4.2  | 3.2 | 3.2  | 2.2 | 0.1 | -    | -   |
| 3.9  | 3.6 | 2.9  | 2.8 | 0.1 | 1.0  | 0.9 |

TABLE V

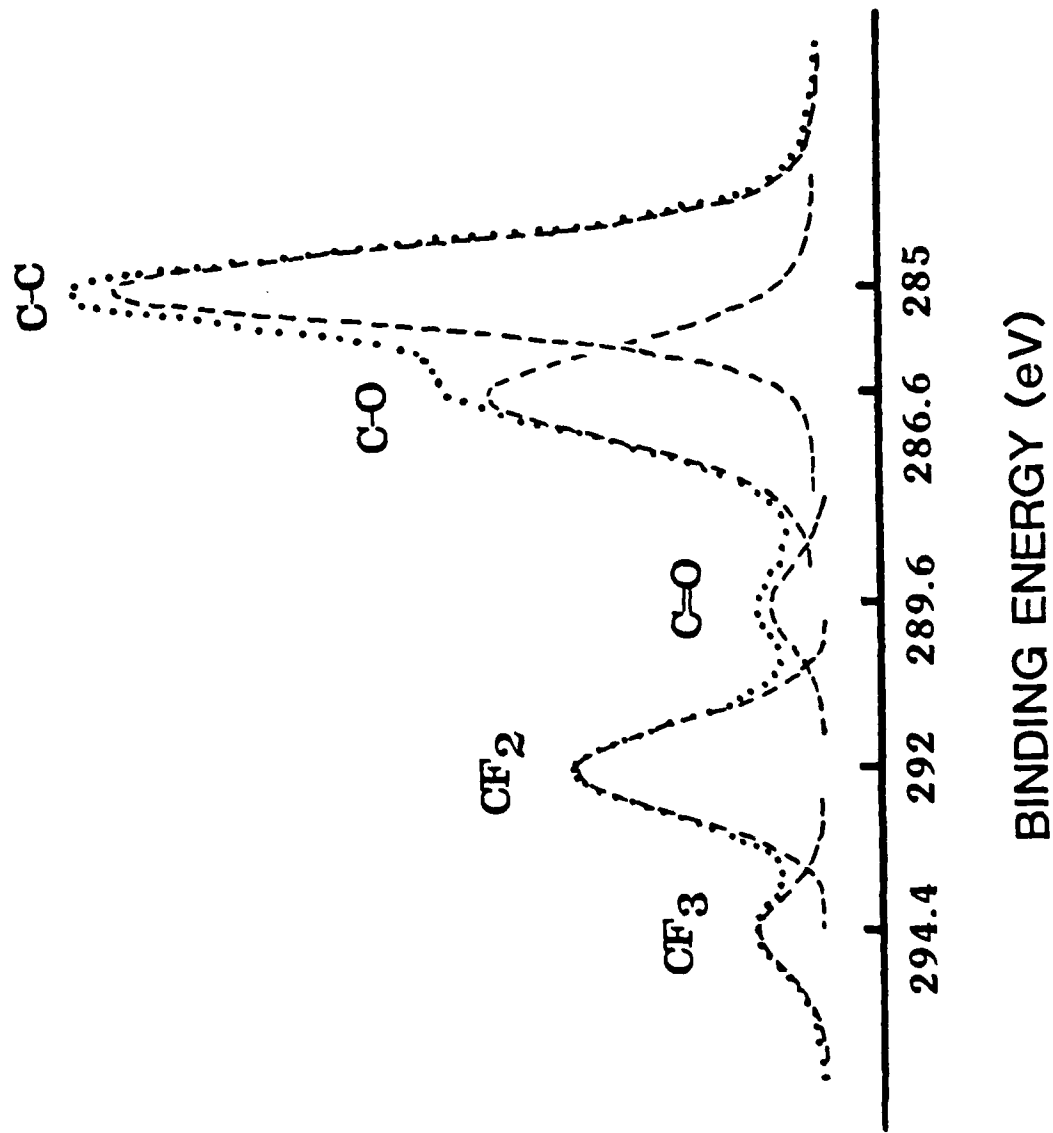
## STATIC AND DYNAMIC CONTACT ANGLE DATA

| Material      | Surface-water-air<br>Contact angle $\pm$ SD | Surface-water-octane<br>Contact angle $\pm$ SD |
|---------------|---|--|
| ET-B33-F0     | 59 $\pm$ 5                                  | 84 $\pm$ 4                                     |
| ET-B33-F4     | 53 $\pm$ 3                                  | 98 $\pm$ 6                                     |
| ET-B33-F9     | 72 $\pm$ 3                                  | 134 $\pm$ 5                                    |
| ET-B33-F14    | 72 $\pm$ 3                                  | 130 $\pm$ 4                                    |
| ET-B33-F9-E08 | 68 $\pm$ 5                                  | 103 $\pm$ 4                                    |
| ET-B50-F50    | 79 $\pm$ 3                                  | 111 $\pm$ 5                                    |
| ET-B33-F67    | 75 $\pm$ 4                                  | 106 $\pm$ 4                                    |
| ET-M34-F66    | 56 $\pm$ 2                                  | 92 $\pm$ 4                                     |
| ET-M34-F66-S8 | 38 $\pm$ 5                                  | 54 $\pm$ 6                                     |

- 48 hours at 25°C

| $\theta_{Adv}$ |         | $\theta_{Rec}$ |         |
|----------------|---------|----------------|---------|
| cycle 1        | cycle 2 | cycle 1        | cycle 2 |
| 80 ± 1         | 80 ± 1  | 49 ± 1         | 48 ± 2  |
| 97 ± 5         | 94 ± 2  | 65 ± 5         | 66 ± 6  |
| 95 ± 3         | 91 ± 2  | 62 ± 6         | 63 ± 7  |
| 102 ± 3        | 98 ± 4  | 62 ± 3         | 62 ± 4  |
| 98 ± 2         | 95 ± 1  | 63 ± 1         | 64 ± 2  |
| 121 ± 2        | 120 ± 2 | 63 ± 6         | 63 ± 5  |
| 123 ± 2        | 117 ± 2 | 34 ± 9         | 31 ± 8  |
| 122 ± 2        | 122 ± 3 | 8 ± 8          | 4 ± 8   |
| 119 ± 2        | 120 ± 1 | 0 ± 0          | 0 ± 0   |

Fig 1



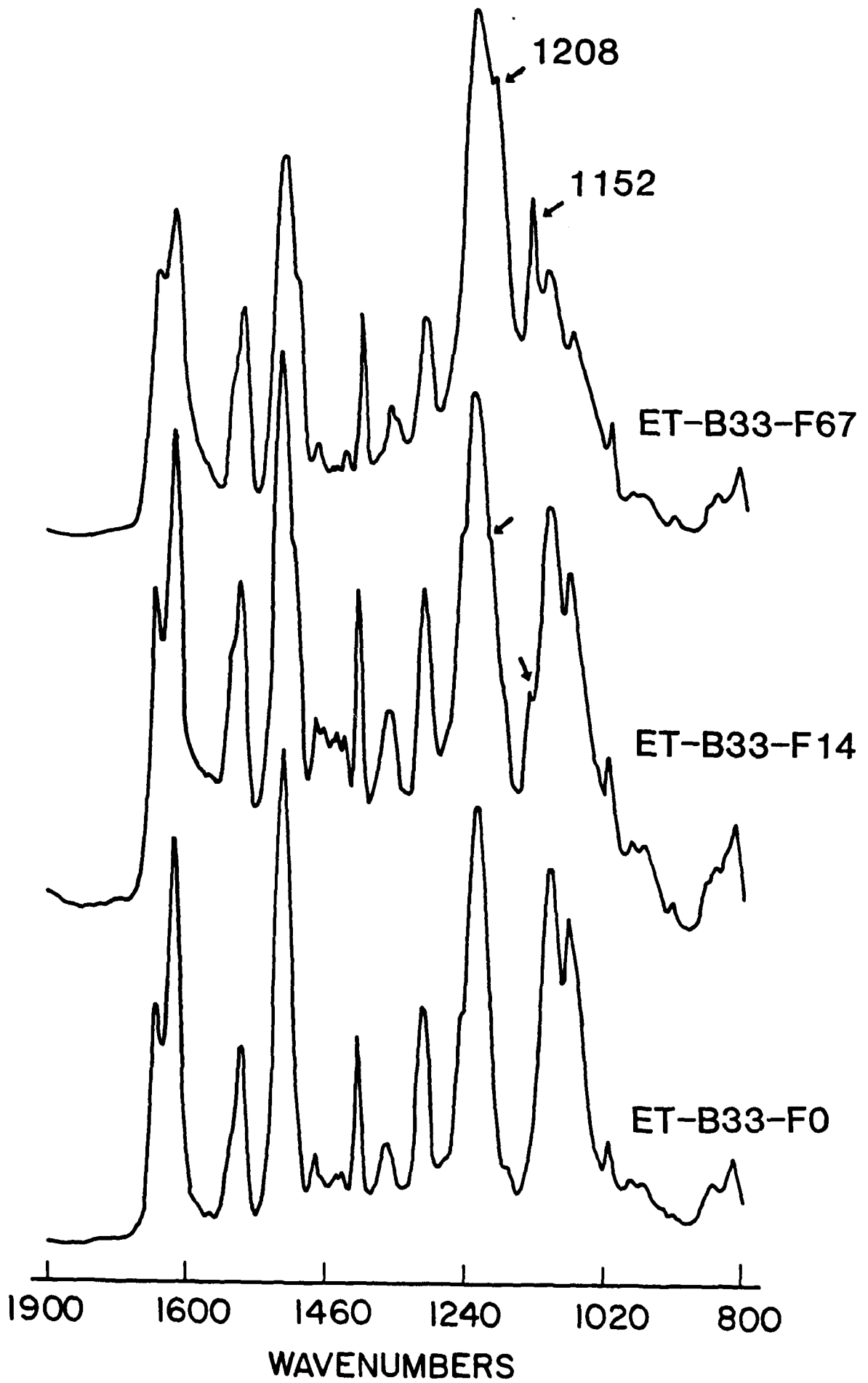
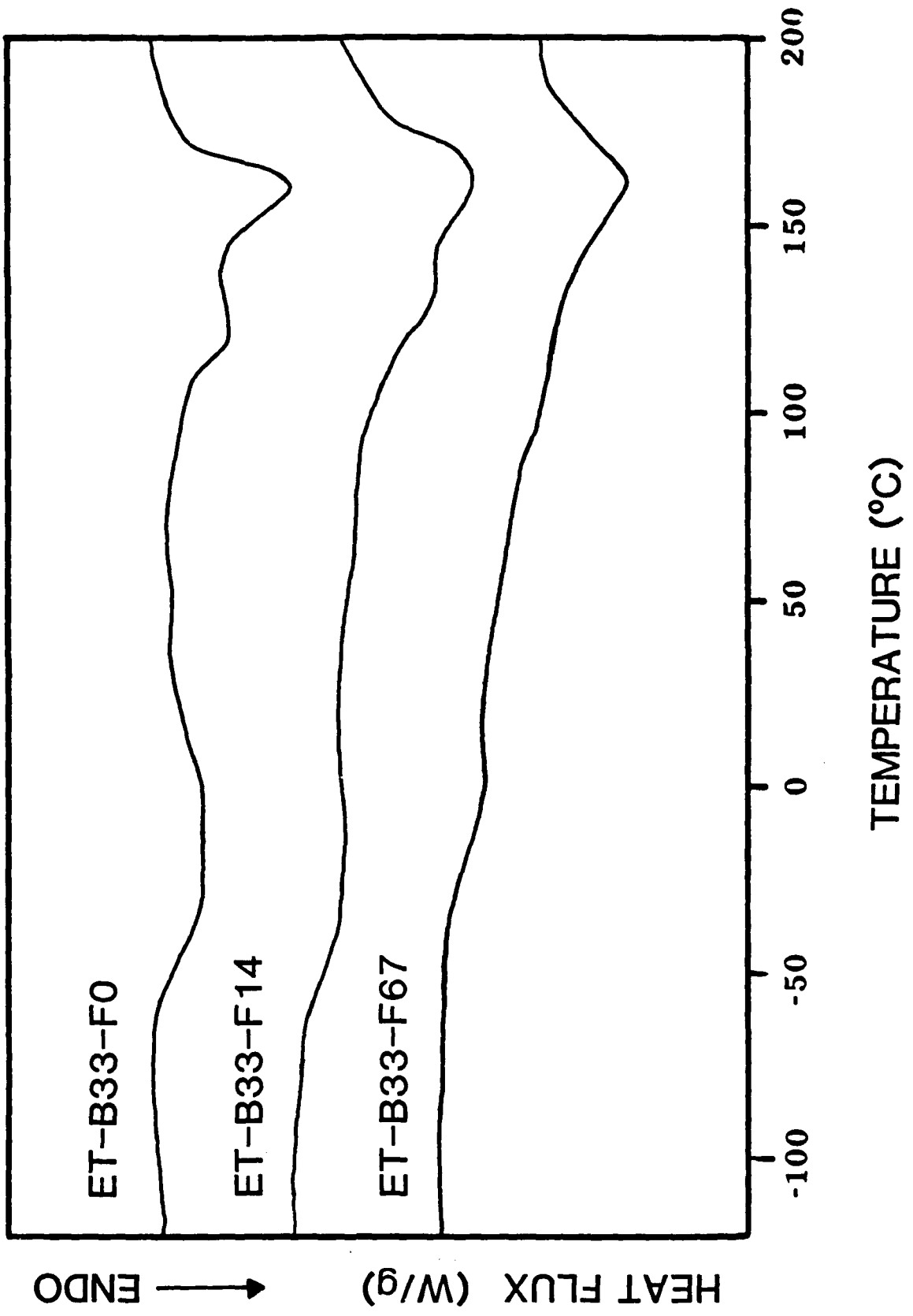


Fig 2

Fig 3



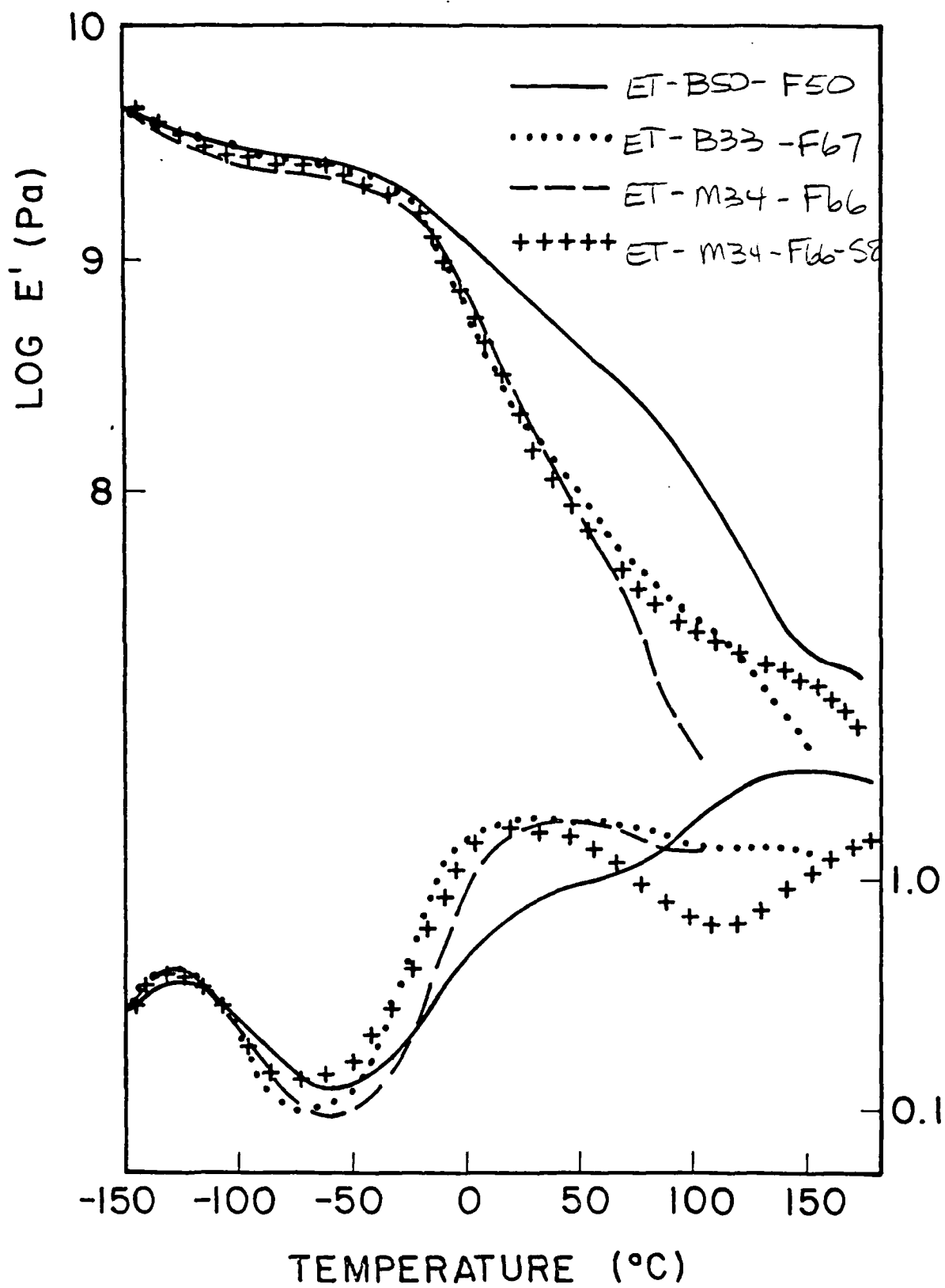
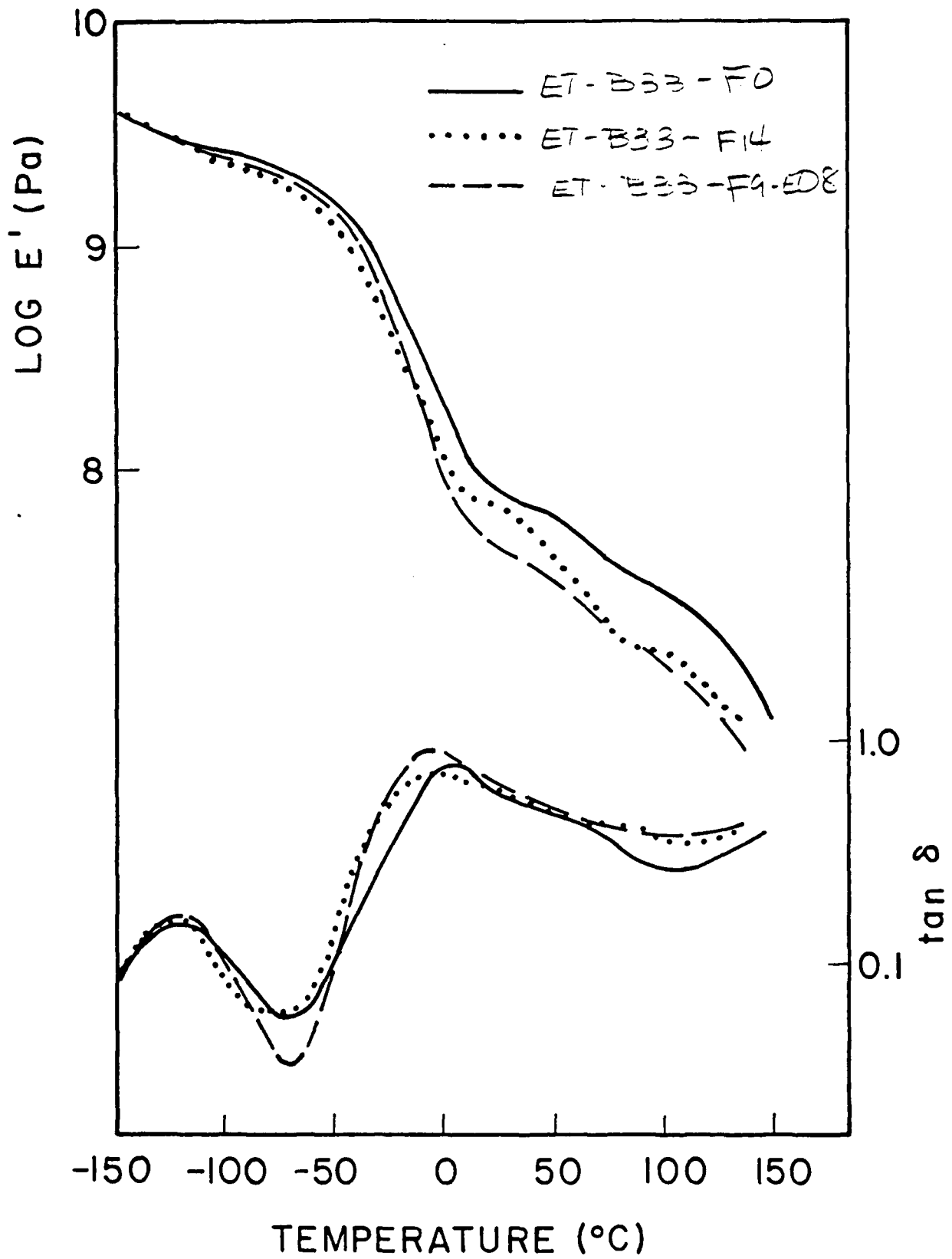


Fig 4



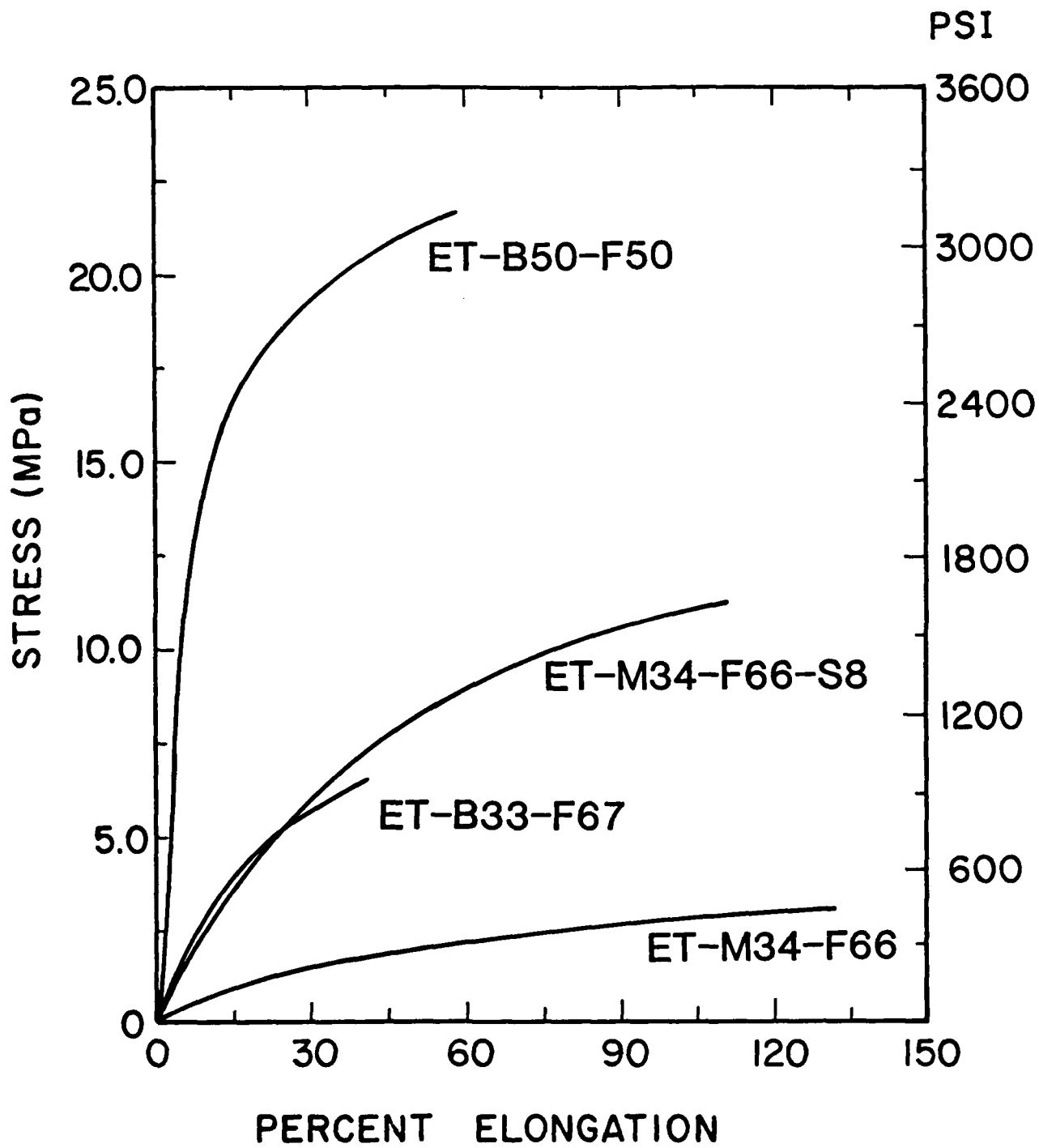


Fig 6

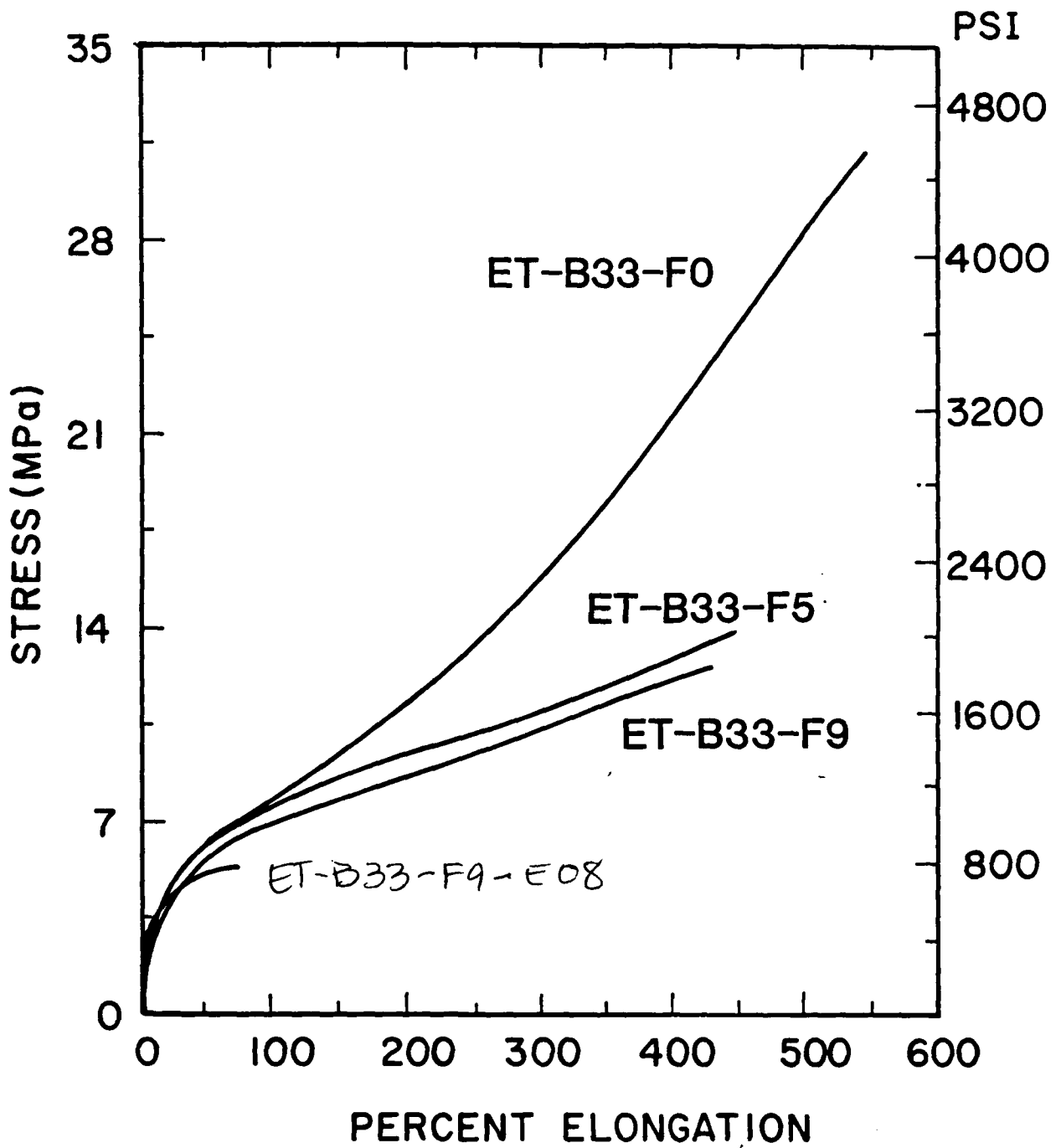


Fig 7